Process Parameter Characterization of Dielectric Elastomer-Based Electro-Mechanical System

Rajeev Kumar and Anuj Kumar Jain

Abstract In recent times, dielectric elastomer-based electro-mechanical system is used widely as actuators and energy harvesters. The material property of elastomer is such that under linear actuations, it can undergo very large deformation. In order to demonstrate large demonstration in actuation, several challenges need to be met. These include the possibility of electro-mechanical instability or electric breakdown and loss of tension in the elastomeric film. In the current work, a material formulation of deformation of soft dielectric material is postulated. Thus, a mathematical model for deformation of dielectric elastomer is created to address processes involved in dielectric elastomer-based energy harvester. Further, the dielectric elastomer material response in tensile testing as well as dielectric permittivity of elastomeric material is evaluated experimentally. The current electro-mechanical model utilizes variation in geometry for change in capacitance which results in storage of more potential at output battery. Efforts are also applied on optimizing the energy harvesting to address various failure situations under electro-mechanical actuations

Keywords Soft dielectric material · Energy harvesting process · Formulation of material response · Electro-mechanical system

1 Introduction

Dielectric elastomers are classified as a class of soft deformable electro-active material, which are also considered as smart materials. This material has got unique mechanical and electrical properties which enable it to stimulate with application of electro-mechanical fields. As a result, dielectric elastomers are considered suitable for various actuations which are observed under electro-mechanical actuators

R. Kumar (✉)
Pranveer Singh Institute of Technology, (Affiliated to AKTU Lucknow), Kanpur, India
e-mail: rajeevnitwkhagoli@gmail.com

A. K. Jain
ABES Engineering College, (Affiliated to AKTU Lucknow), Ghaziabad, India
e-mail: anujjainkanbay@gmail.com

P. Joshi et al. (eds.), *Advances in Engineering Design*, Lecture Notes in Mechanical Engineering, https://doi.org/10.1007/978-981-33-4684-0_70

and energy harvesters. Especially for applications requiring large actuation at high voltage and low cost, dielectric elastomers provide a lightweight alternative to other technologies. Most dielectric elastomer actuator designs were developed during the early 2000s [1, 2]. Further application of this technology as a buoy generator and a heel strike generator has been reported [3]. Practical self-priming circuits, that boost the low-voltage source so that dielectric elastomer generators (DEGs) can harvest energy effectively, have been developed [4].

The general problem of a soft dielectric material undergoing large deformations due to the application of an electric field is the one that assumes renewed interest in the light of the emergence of technologies based on dielectric elastomers. Factors limiting the application of these emerging technologies are many. During usage, as very high electric field is required for deforming these elastomers, hence possibility of electric breakdown and electro-mechanical instability is the most common concern [5–7]. In order to understand these concerns, the basic working of elastomer-based actuators should include important parameters during electro-mechanical deformations.

Consider the case of the thin elastomer between compliant electrodes as shown in Fig. 1. This is a generic configuration adopted in many applications. When a voltage φ is applied on an unconstrained dielectric film, its thickness decreases. The decrease in thickness induces a higher electric field and hence, a higher compressive Maxwell stress, which, in turn, thins it further. At a critical point, the positive feedback may cause the dielectric to thin down abruptly, leading to, what is known as 'pull-in instability.' Wrinkling of the film is commonly observed during pull-in instabilities. Hence, in order to address these failure situations, various parameters influencing

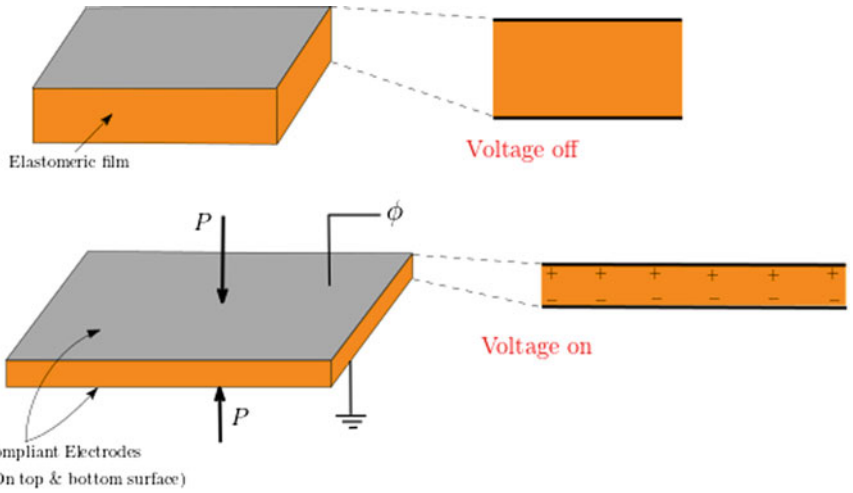

Fig. 1 Schematic diagram showing working principle of dielectric elastomer. When electric charges are placed over an elastomer thin sheet, coated on both sides with compliant electrodes, electrostatic forces, P acts to squeeze the film along thickness direction and expands it in plane

the deformation process need to be highlighted for which a mathematical model is required.

2 Theory of Deformable Dielectric Elastomer

In this section, the equations governing the deformation behavior of highly deformable nonlinear elastic dielectric materials under the coupled influence of mechanical and electric fields are derived. The situation is shown in Fig. 2, where a point P with position vector X in the reference configuration of a solid body V_o^+ is mapped to point p with position vector x in the deformed configuration denoted V^+ by a motion $x = \beta(X, t)$. The body is subjected to a body force distribution $B(b)$ in the reference(deformed) configuration over $V_o^+(V^+)$ and mechanical surface tractions $T(t)$ applied on a part of the boundary $\partial V_0^+(V^+)$ with $N(n)$ being normal to the surface. In addition, the body has a material (spatial) distribution of free charge per unit volume $\dot{Q}(X, t)$ $(q(x, t))$, as well as charge per unit area $\omega_o(\omega)$ per unit surface area $\partial V_0(V)$. The deformable dielectric body is embedded in an electric field $\dot{E}(X, t)$ in the reference or $E(x, t)$ in the deformed configuration. The reference and deformed configuration are both embedded in free space, $(V_0)^-$ and $V,^-$ respectively. The outer boundary of the free space lies far away, and all field quantities decay to zero there.

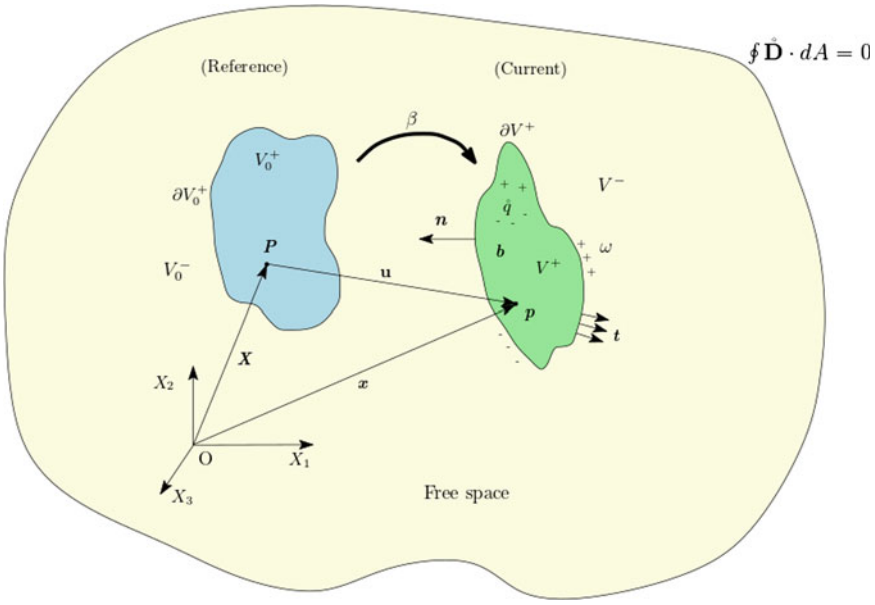

Fig. 2 General electro-mechanical loadings on deformable dielectrics

Here, the development of equations governing electro-mechanical deformations is casted in reference configuration. In the reference configuration, the electric field $\dot{E}(X)$, potential $\dot{\varphi}(X)$, electric displacement $\dot{D}(X)$ and surface charge density ω_o are connected through Maxwell's equations:

$$\dot{E} = -\frac{\partial \dot{\varphi}}{\partial X}, \tag{1}$$

$$\nabla_0 \cdot \dot{D} = \frac{\partial \dot{D}_i}{\partial X_i} = \dot{Q}, \tag{2}$$

in $V_o = V_o^+ \cup V_o^-$ and the jump condition on ∂V_o^+,

$$\left\| \dot{D} \cdot N \right\| = \omega_o. \tag{3}$$

Here, N is the outward normal to the surface ∂V_o^+ in the fixed Cartesian system(X_1, X_2, X_3). Further, $\|\cdot\|$ implies a jump in a quantity across surface, so that $\left\| \dot{D} \right\| = \dot{D}^- - \dot{D}^+$, with N always taken to point from the + side to the - side. The above shown constitutive relation between $\dot{E}$ and $\dot{D}$ in the reference configuration is through a deformation-dependent permittivity tensor. The deformation gradient, Jacobian of the deformation and the right Cauchy–Green deformation tensor are given by the usual relations:

$$F = \frac{\partial x}{\partial X}, \; J = \det F \text{ and } C = F^T F \tag{4}$$

Principle of conservation of linear momentum for quasi-static condition is expressed as:

$$\int_{V_o^+} \left(B + B^E\right) \mathrm{d}V_o^+ + \int_{\partial V_o^+} \left(T + T^E\right) \mathrm{d}S_o = 0, \tag{5}$$

where the left-hand side envisages that the body forces and surface tractions, acting on the deformable body, have mechanical and electrostatic origins. The quantity B and T are usual mechanical body force and traction, while B^E and T^E are corresponding electrostatic load components for body force and traction, respectively. Toupin [8] related the electric body force to Maxwell's stress using

$$B^E = \nabla_o \cdot P^E, \tag{6}$$

leading to traction $T^E = \left\| P^E \right\| N$ on ∂V_o^+. As per [9], relation between surface traction and jump in total nominal stress is given by: $T = \left\| P + P^E \right\| N$.

After performing few manipulations and utilizing expression of electric traction in terms of Maxwell stress P^E, we are expressing here the localized equation describing balance of linear momentum as:

$$(\nabla_o \cdot P) + \left(B + B^E\right) = 0, \tag{7}$$

where P is the first Piola-Kirchhoff stress.

For an isotropic and isothermal material undergoing deformation, Helmholtz's free energy density is considered to constitute deformation gradient as well as electric displacement and is shown of form:

$$\widetilde{\Upsilon} = \overline{\Upsilon}\left(F,\ \dot{D}\right) \tag{8}$$

Further constitutive relations are considered into two parts, one with pure mechanical component, while other consisting of electro-mechanical parts as shown below:

$$P + P^E = \frac{\partial \widehat{\Upsilon}}{\partial F}, \tag{9}$$

$$\dot{E} = \frac{\partial \dot{\widehat{\Upsilon}}}{\partial D} \tag{10}$$

3 Mathematical Modeling of Elastomer-Based Energy Harvester

A dielectric elastomer is basically a soft hyperelastic material with a reasonably high dielectric permittivity ε. Dielectric elastomeric generator (DEG) has been shown to exhibit favorable energy densities, when used for energy harvesting, e.g., in heel strike generators and harvesters from ocean. The example worked out in this section closely follows their derivation in previous section. The stages in the operation of a DEG are shown in Fig. 3. A thin sheet of elastomer, a 3 M, VHB 4910, with thickness L_3, is used at computational mechanics laboratory, IIT Kanpur, with flexible electrodes at $X_3 = 0$, and L_3. It is bi-axially stretched to a stretch of λ_m in the process (a)–(b). The stretch is held fixed from (b)–(c), while charges $\dot{Q}_m$ are transferred to the electrodes from ϕ_{in}. In (c)–(d), switches S_1 and S_2 are opened so that the charges cannot escape. The elastomer is relaxed to $\lambda = 1$. Finally, in the process (d)–(a), the switch S_2 is closed so that charges are transferred to ϕ_{out}. If $\phi_{\text{out}} > \phi_{\text{in}}$, the process has been able to transfer charge from a lower to a higher potential and thus converted the mechanical energy of stretching to stored electrical energy in ϕ_{out}.

For hyperelastic material, free energy density is considered as:

$$\overline{\Upsilon} = \underbrace{\breve{\Upsilon}\,(\mathrm{C})}_{\text{mechanical}} + \underbrace{\widehat{\Upsilon}(C,\ \dot{D})}_{\text{electro-mechanical}}, \tag{11}$$

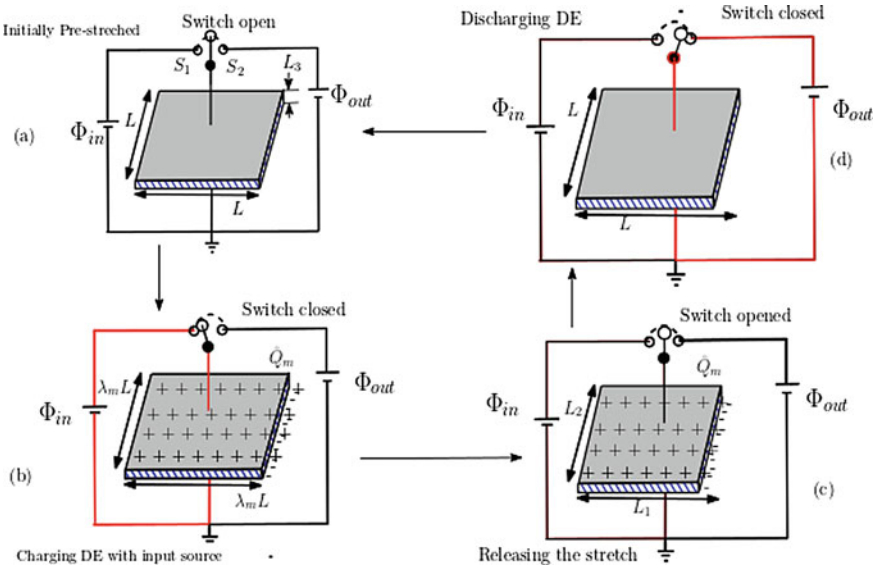

Fig. 3 A parallel plate capacitor, with hyperelastic dielectric elastomer and flexible electrodes, acts as a dielectric elastomeric generator (DEG). Stages of operation: **a** through **d**

where electro-mechanical component is given by $\widehat{\Upsilon}(C,\ \dot{D}) = \frac{\dot{D}\cdot C\cdot \dot{D}}{2\varepsilon J}$. Apart from this, hyperelastic material elastomer behaves nearly as impressible material; hence, constitutive relation can be shown as:

$$P + P^E = \frac{\partial \overline{\Upsilon}}{\partial F} - p_o F^{-T}, \tag{12}$$

where p_o is called as Langrage multiplier. In case of DEG, we have assumed the energy density functions to be depending upon principle stretches as well as reference electric displacement. Here, the constitutive relation gets modified as:

$$P_\alpha + P_\alpha^E = \left[\frac{\partial \breve{\Upsilon}}{\partial \lambda_\alpha} + \frac{\partial \widehat{\Upsilon}}{\partial \lambda_\alpha}\right] - \frac{p_o}{\lambda_\alpha} \tag{13}$$

where $\breve{\Upsilon}(\lambda) = \frac{\mu_1}{\alpha_1}\left[\lambda_1^{\alpha_1} + \lambda_2^{\alpha_1} + \lambda_3^{\alpha_1} - 3\right]$ and $\breve{\Upsilon} = \breve{\Upsilon}(\lambda_1,\ \lambda_2,\ \lambda_3,\ \mathbf{D})$. Here, coefficients $\mu_1 = 29.54$ kPa and $\alpha_1 = 1.615$. Dielectric permittivity $\varepsilon = 4.832 \times 10^{-11}\left(\frac{F}{m}\right)$. All these values are calculated for VHB 4910, by undergoing tensile testing at Aerospace Engg. Laboratory, IIT Kanpur. Now, all the four stages in DEG are formulated using the above defined constitutive relations. The initial elastomer sheet is square with $L_1 = L_2 = 40$ mm and $L_3 = 1$ mm. When the free energy is given in terms of principal stretches, eq. (12) gets transformed as:

$$\frac{\partial \breve{\Upsilon}}{\partial \lambda_\alpha} = \frac{\lambda_\alpha \dot{D}_\alpha^2}{\varepsilon J} - \frac{1}{2\varepsilon J}\frac{\partial J}{\partial \lambda_\alpha}(\lambda_i^2 \dot{D}_i^2) \tag{14}$$

In case of the DEG, using the Ogden model and equi-biaxial stretches so that $\lambda_1 = \lambda_2 = \lambda$; incompressibility further dictates that $\lambda_3 = 1/\lambda^2$. Also $D_3 \neq 0$, $D_1 = D_2 = 0$, we get:

$$P = P_1 + P_1^E = P_2 + P_2^E = \mu_1 \lambda^{\alpha-1} - \frac{\dot{D}_3^2}{2\varepsilon\lambda^5} - \frac{p_o}{\lambda}, \tag{15}$$

$$P_3 + P_3^E = \mu_1 \lambda^{-2\alpha_1+2} + \frac{\dot{D}_3^2}{2\varepsilon\lambda^2} - p_o\lambda^2. \tag{16}$$

As per traction boundary condition, total nominal stress acting on top and bottom surfaces is vanished. Hence, $P_3 + P_3^E = 0$ is considered throughout the operating cycle. Therefore, $p_o = \mu_1 \lambda^{-2\alpha_1} + \frac{\dot{D}_3^2}{2\lambda^4}$. Now, inserting value of p_o in expression of P, we get:

$$P = \mu_1\left[\lambda^{\alpha_1-1} - \lambda^{-2\alpha_1-1}\right] - \frac{\dot{D}_3^2}{2\varepsilon\lambda^5} \tag{17}$$

Further, the electrostatic constitutive relation is given as:

$$D_3 = \varepsilon\lambda^4 \dot{E}_3\,. \tag{18}$$

Equations (17) and (18) can now be used to plot the entire cycle on the $P - \lambda$ and $E_3 - \dot{D}_3$ plane. Note that as $\dot{D}_3 = \frac{\dot{Q}}{L^2}$, and $\dot{E}_3 = \frac{\dot{\phi}}{L_3}$. where $\dot{Q}$ is the charge transferred to the electrodes and $\dot{\phi}$ is the potential applied, then $E_3 - \dot{D}_3$ plot becomes equivalent to $\dot{\phi} - \dot{Q}$ plot.

For process (a)–(b), the deformation gradient is given as:

$$F = \lambda \mathrm{e}_1 \otimes \mathrm{e}_1 + \lambda \mathrm{e}_2 \otimes \mathrm{e}_2 + \frac{1}{\lambda^2}\lambda \mathrm{e}_3 \otimes \mathrm{e}_3, \tag{19}$$

where λ varies from 1 to $\lambda_m = 4$, and $\dot{D}_3 = 0$. The complete process from (a) to (d) is shown in Figs. 4, 5, respectively. Further, ϕ_m is varied here for the VHB 4910 elastomer having thickness of 1 mm. Maximum value of voltage applied is 1 kV for a fixed stretch of $\lambda_m = 4$ during process (b)to (c). Further at point (d), the negative stress is undesirable as it might cause loss of tension. The point (d) lies outside the limits of this plot and so, is indicated by an arrow in Figs. 4, 5, respectively.

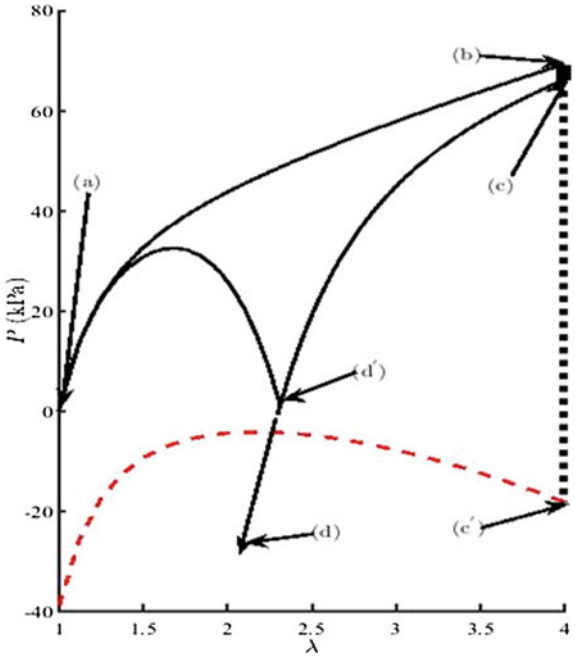

Fig. 4 Nominal stress versus stretch plot

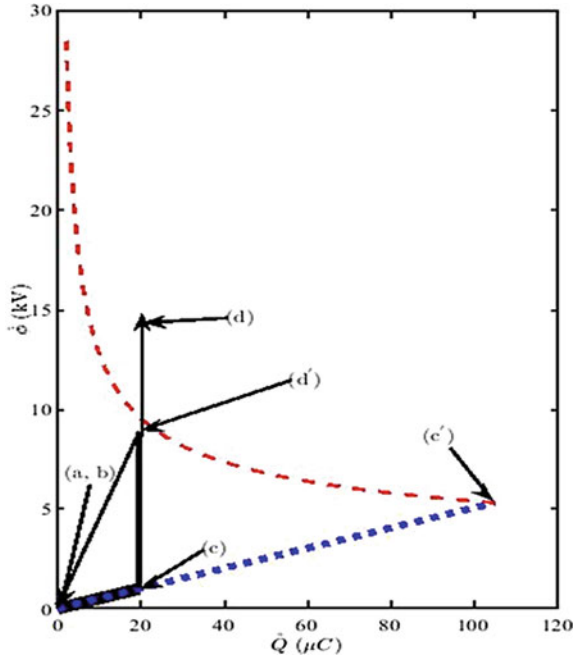

Fig. 5 Voltage–charge plot for no failure

3.1 Limits on $\dot{Q}_m$

The process from (b)–(c) involves loading the elastomer with charge. At $\lambda_m = 4$, $\dot{\phi} = 1\,kV$, the charge that can be loaded onto the DE capacitor is $\dot{Q}_m = 19.8\,\mu C$. However, the maximum charge that can be loaded onto the capacitor at stage (c) is limited by the breakdown characteristics of the DE material. The breakdown field varies with stretch, and for the purpose of the following calculations, we consider a fit to experimental data of the form: $E_B = -0.16667\,\lambda^3 + 2.5257\lambda^2 + 9.7024\lambda + 16.4$.

Further, we have tried to include electric breakdown field expression in $P - \lambda$ plane and $\dot{\phi} - \dot{Q}$ plane respectively as:

$$P = \mu_1\left[\lambda^{\alpha_1 - 1} - \lambda^{-2\alpha_1 - 1}\right] - \frac{\varepsilon E_B^2}{\lambda}, \text{ and } \dot{D}_3 = \varepsilon\lambda^2 E_B. \tag{20}$$

These plots are shown as dotted lines in red, which limits the extent for charge on stretched elastomer. For a practical dielectric elastomer generator device, it is now clear that we follow $\dot{\phi} = 1kV$ and de-stretch up to (d') and then de-stretch and discharge at the same time along the curve (d')–(a) as shown in Figs. 4 and 5. The combined relaxation and discharging process should be done in a manner such that the curve from (d') to (a) does not cross the breakdown curve and does not lead to negative value of P. The point (d') has been chosen such that neither loss of tension nor electrical breakdown occurs anywhere in the domain. The bow-shaped curve from (d') to (a) shown in Fig. 4 is near to realistic, where we have chosen (d') to have stress very close to 0. It is more practical to move (d') to a higher value of λ.

4 Conclusion

In the present work, constitutive relations using material coordinates for deformation of elastomeric material under both electrical and mechanical load are postulated. Based on the derived constitutive relation, a suitable mathematical model is envisaged, and its working is shown. Further, various points on stretch and stress plot are drawn during deformation process. Corresponding situations are also shown at voltage charge graph. These two characteristic plots determine the influencing positions during deformation of elastomer. Limits of failure points are also ascertained, which provide a glimpse of necessary action to be used while designing a prototype dielectric elastomer-based energy harvester.

References

1. Kornbluh RD, Eckerle J, McCoy B (2011) A scalable solution to harvest kinetic energy. In SPIE Newsroom
2. Pelrine R, Kornbluh R, Eckerle J, Jeuck P, Oh S, Pei Q, Stanford S (2001) Dielectric elastomers: generator mode fundamentals and applications. Proc SPIE Smart Struct Mater 4329:148–156
3. Prahlad H, Kornbluh R, Pelrine R, Stanford S, Eckerle J, Oh S (2005) Artificial muscle: the next generation of robotic actuators. In: Proceedings of the ISSS, Bangalore, India, 28–30, July 2005
4. McKay T, O'Brien B, Calius E, Anderson I (2010) Self-priming dielectric elastomer generators. Smart Mater Struct 19:055025
5. Huichan Z, Aftab MH, Mihai D, Daniel MV, Robert JW, David RC (2018) Compact dielectric elastomer linear actuators, Advanced functional materials, vol 1804328, pp 1–12. https://doi.org/10.1002/adfm.201804328
6. Duduta M, Hajiesmaili E, Zhao H, Wood RJ, Clarke DR (2019) Realizing the potential of dielectric elastomer artificial muscles. PNAS. https://doi.org/10.1073/pnas.1815053116
7. Minaminosono A, Shigemune H, Okuno Y, Katsumata T, Hosoya N, Maeda S (2019) Deformable motor driven by dielectric elastomer actuation and flexible mechanisms. Front Robot AI. https://doi.org/10.3389/frobt.2019.00001
8. Toupin RA (1963) A dynamics theory of elastic dielectrics. Int J Eng Sci 1:101–126
9. McMeeking RM, Landis CM (2005) Electrostatic forces and stored energy for deformable dielectric materials. J Appl Mech ASME 72:581–590